Reprinted from

Symposium on

Machine Processing of

Remotely Sensed Data

June 3 - 5, 1975

The Laboratory for Applications of
Remote Sensing

Purdue University
West Lafayette
Indiana

IEEE Catalog No.
75CH1009-0 -C

SUMMARY OF : PHOTOGRAPHIC DISPLAY OF LANDSAT-1 CCT IMAGES FOR IMPROVED GEOLOGICAL DEFINITION

Longshaw T.G.*, Viljoen R.P.*, and Hodson M.C.+

* Johannesburg Consolidated Investment Company Limited
Fundamental Research Department
P.O. Box 590
Johannesburg, South Africa.

+ National Institute of Telecommunications Research of
Council for Scientific and Industrial Research
P.O. Box 3718
Johannesburg, South Africa

ABSTRACT

LANDSAT-1 Bulk MSS Computer Compatible Tapes (CCT's) maintain the intrinsic radiometric and spatial qualities of the MSS (NASA, 1972) and as such are potentially superior to MSS 70 mm photographic products in the study of both regional and small scale geological trends. A convenient method of realising this potential is via a digital-to-analogue conversion of processed CCT data and CRT display to produce photographic hardcopy. This paper describes a flexible method of producing such displays that can be colour composited with ground-based mapping data transformed to be compatible with the MSS geometric projection. Mapping accuracy of image detail to corresponding ground features was of the order of 50 to 160 meters rms over individual CCT areas of image 1049-07301. Two geological applications of CCT imagery are described and in each case the improved geological definition of CCT displays over that obtainable from NASA 70mm transparencies is illustrated.

INTRODUCTION

LANDSAT-1 MSS Computer Compatible Tapes (CCT's) offer a flexible tool to the user in which spatial and radiometric quality is potentially superior to that of the NASA photographic product (NASA, 1972). Automatic interpretation techniques have been used extensively in the study of MSS CCT imagery and employ the well established principles of computer data processing (Lars, 1967; Nagy, 1968). A problem encountered in automatic interpretation of CCT's is suitable display of processed image data. A LANDSAT frame contains some 24 million bytes of video data and presentation of processed pixel values in their correct spatial format can produce voluminous hard copy. In this respect, the NASA photographic product has an advantage over the CCT format as the packing density of information on a film emulsion is much greater than that obtainable from standard computer peripherals.

In geological applications this is an important consideration as image analysis techniques are geared to the manual observation of compact high-resolution hardcopy that maintains synoptic coverage. A useful method of combining the advantages of the two formats therefore is to display the output of CCT image processing in photographic form. The method described here employs hardware commonly used in present-day data processing and remote sensing and achieves image quality comparable with dedicated systems. The generation of the method was motivated by a need for improved geological definition from presently available LANDSAT-1 imagery in specific geological problem areas.

This necessitated a reproduceability of scale for each CCT display in a frame in order to maintain image definition in colour composites. In producing such composites it was desirable to include ground truth overlays which were spatially compatible with their corresponding CCT displays. This entailed the transformation of ground correlation data from national maps (produced as conformal projections) to suitably scaled overlays in the geometrical projection of the MSS.

Although some of the concepts involved in this CCT technique have been expressed previously (Vincent, 1973; McEwan and Asbeck, 1975) methods of implementing such concepts in a practical approach to geological exploration have not been in evidence. This presentation is therefore concerned with the operational aspects of this particular CCT display method, ground truth overlay accuracy, and illustrations of the improved geological definition obtainable from MSS CCT displays over Bulk MSS 70mm transparencies. As specific examples of the latter, two geological applications of CCT displays are described in detail with particular reference to the tangible benefits derived from their photointerpretation in geological exploration programs.

METHOD

The photographic display of CCT imagery was achieved using a Hewlett-Packard minicomputer with a 100kHz digital-to-analogue conversion facility, an FM analogue tape recorder and a linescan film recorder. The HP mini used 9 track Bulk MSS CCT's which were accessed using an assembler-level language subroutine. The transfer of each linescan segment into memory was initiated by the leading edge of a sync pulse (frequency f_1). During one cycle of the sync pulse, the CPU appropriately processed each spectrally interleaved pixel group of the scan line according to a predetermined function and returned the result to memory. On the successive sync pulse leading edge, program control sequentially output the result of each pixel computation in order of linescan through the 8-bit D-to-A device. This output was regulated by an external clock pulse (of frequency $f_2 \simeq 2f_1.IXL$, where IXL was the number of MSS pixels in each CCT video record) which produced the sync pulse via a counter in the computer program. The sync pulse in turn gated the clock pulse train to enable the D-to-A conversions. Initiating the clock pulse train in this manner improved image reproduction in the scan advance direction as each computed pixel value appeared in the same position along the waveform as its corresponding pixel in any other linescan record. As the HP computer was relatively slow (only 10 linescan segments per second under program control) the analogue waveforms from the D-to-A (plus the sync pulse) were FM recorded on a Sangamo Sabre III tape recorder at 7½ ips. The tape recorded waveforms were then played back off-line at 60 ips into a Texas Instruments RFR-70 linescan film recorder which had a minimum sweep rate of 50 linescans per second. The analogue data were thereby exposed as video records on Kodak 2479 70mm recording film by imaging a repetive CRT sweep (driven by the recorded sync pulse), which was Z-modulated with the CCT analogue signal. The recording film was then photographically processed to yield the CCT image. As each CCT comprising an MSS frame was processed individually, each display covered only a quarter of the full frame.

OPERATIONAL DETAILS

Operational details included the output of each record through the D-to-A device twice so that by reducing film transport rate in the CRT image plane by a factor of two, image quality could be improved by overscanning. D-to-A output was 0.0 volts (all zero bits) to 1.0 volts (all bits set). The film recorder was AC coupled and used a sample and hold circuit to extract a DC reference voltage from the first 70 µs of the video waveform. This DC level was restored to the signal prior to driving the CRT grid. A 0.5 volt DC level was therefore output for a period of 1ms prior to each D-to-A data burst. The gain and DC level could be adjusted as required in the tape-recording playback in order to increase or decrease contrast and bring either low or high pixel output values into the 0,4 to 1,3 density range of the film. In this way, the radiometric accuracy of the CCT which was compromised in a low contrast image, could be adequately displayed in high contrast playbacks at different DC levels. As the film recorder could accept sync

pulse durations from 1,4ms to 10ms to produce the sweep drive, "windows" of arbitrary dimensions could be extracted from the analogue recorded image and "stretched" to the full 70mm format of the film recorder. This was done by simply triggering a pulse generator with the playback sync pulse, adjusting the delay and width of the triggered pulse to correspond to the appropriate section of the video waveform and using it to drive the CRT sweep. For purposes of subsequent data superimposition, fixed records were output through the D-to-A device before and after each CCT run to produce registration crosses on the film display.

From the above description it can be seen that the method is flexible and accommodates the photographic display of any systematic pointwise computation of the CCT pixel matrix. Displays of individual bands and ratio images have been significantly more informative than have prints derived from NASA photographic products. This is no doubt partly due to the fact that the latter product as received by the user is 3rd or 4th generation from NASA's Electron Beam Recorder (EBR) whereas a CCT display is effectively first generation and is produced in a larger format from the CRT than that from the EBR. Although the method caters for the film display of spectral recognition function output values, such images have not yet yielded information that could not otherwise be extracted from band/ratio colour composites images. However, this could possibly be due to the qualitative approach presently adopted in determining appropriate spectral recognition functions.

COLOUR COMPOSITIONING DISPLAYS

One of the most useful properties of this type of CCT technique is that combinations of individual bands/ratio images (recognition functions) can be photographically colour composited to aid correlation of differing spectral/spatial information. This can be achieved by several runs of the program for a particular CCT under identical conditions (clock frequency, film transport speed etc.) and appropriately changing the pixel function from run to run. In this manner, several black and white negatives were produced which could be spatially registered. The negatives were then photographically enlarged X2 onto Kodak 4133 to produce high-contrast positive separations which were then registered and punched. These separations were then placed on register pins overlaying Agfa D13 Duplichrome on an enlarger baseplate and exposed sequentially through Wratten 98, 99 or 29 filters depending on whether the separation image was required to appear as blue, green or red in the subsequent colour print. Standard colour processing of the Duplichrome gave a master positive from which colour prints (Cibachrome P10) could be conventionally produced (Kreitzer, 1974). While producing spatially registered displays from the same CCT image was comparatively simple, accurate superimposition of detailed ground truth maps was more involved.

SUPERIMPOSITION OF GROUND TRUTH

Having produced CCT displays from which conventional photointerpretation could be applied, it was desirable to accurately relate interpreted features to ground truth. Specifically, stratagraphic and structural detail noted on the CCT displays was required to be overlain directly by base maps. In this way, the significance and positioning of interpreted features could be assessed in relation to their geological setting and the imagery could be scrutinized for fine lithological features intervening the more obvious stratagraphic units which might have otherwise been overlooked. This subjective feed-back approach to interpreting LANDSAT images relied on the registration of the CCT displays with ground truth overlays to the order of one or two pixels. As the CCT displays were in the skew pseudo-perspective projection produced by the MSS scanning mode and base maps were produced in a conformal projection, it is necessary to set up a mathematical correspondence to portray the data of one in the projection of the other. A convenient method of setting up this mathematical correspondence is to use a first or second order polynomial transformation respectively of the form,

$$x = a_0 + a_1u + a_2v$$
$$y = b_0 + b_1u + b_2v \qquad (1)$$

or

$$x = a_0 + a_1u + a_2v + a_3u^2 + a_4v^2 + a_5uv$$
$$y = b_0 + b_1u + b_2v + b_3u^2 + b_4v^2 + b_5uv \qquad (2)$$

Where (x,y) is the pixel location in the CCT matrix in the byte advance (x) and scan advance (y) directions and (u,v) are the equivalent ground co-ordinate expressed in a rectangular cartesian grid overlaying a conformal projection.

The use of affine and higher order transformations in evaluating the cartographic qualities of ERTS-1 imagery has been described by several authors notably, Skoomaker (1974), Colvocoresses (1974) and McEwan (1975). These studies were concerned with the cartographic qualities of MSS imagery as a source of geometrically undistorted maps. The present study differs slightly in that it is concerned with the transformation of base map features for photographic composition with CCT displays. In this exercise, base maps were expressed in a Gauss Conform or Transverse Mercator projection and the (u,v) co-ordinates of equation (1) and (2) expressed in the South African National Co-Ordinate system in units of 10,000 feet with a predetermined meridian/equator intersection as origin (depending on longitude location). In order to implement the transformations, it was necessary to evaluate the (a_n,b_n) co-efficients using a set of control points. These control points were chosen by relating high-contrast features in a CCT photographic display of MSS band 5 (or 7) to ground features on 1:50 000 Topographic maps. Prominent detail within the ground features were then related (with the aid of aerial photographs) to a high/low pixel value

boundary using appropriate computer printout of the area. As the detail was generally irregular in shape, vertices were common and a "most probable pixel" could be identified as the corresponding CCT co-ordinate. This aspect of the method was a limiting factor on the accuracy of the method however as it was difficult to estimate the (x,y) coordinate better than to an integer pixel with any degree of certainty. This was in contrast to sub-pixel location accuracy reported in a study of 1st generation NASA positives (McEwan and Asbeck, 1975).

Having set up a number of (x,y,u,v) control points evenly distributed over the image area concerned, the (a_n, b_n) co-efficients were calculated using a least squares method. This involved the evaluation by computer program of the respective deterministic expressions from equations (1) and (2), namely:

$$\begin{vmatrix} N & \Sigma u_2 & \Sigma v \\ \Sigma u & \Sigma u & \Sigma uv \\ \Sigma v & \Sigma uv & \Sigma v^2 \end{vmatrix} \begin{vmatrix} a_0 \\ a_1 \\ a_2 \end{vmatrix} = \begin{vmatrix} \Sigma x \\ \Sigma ux \\ \Sigma vx \end{vmatrix} \quad (3)$$

and

$$\begin{vmatrix} N & \Sigma u & \Sigma v & \Sigma u^2 & \Sigma v^2 & \Sigma uv \\ \Sigma u & \Sigma u^2 & \Sigma uv & \Sigma u^3 & \Sigma uv^2 & \Sigma u^2v \\ \Sigma v & \Sigma uv & \Sigma v^2 & \Sigma u^2v & \Sigma v^3 & \Sigma uv^2 \\ \Sigma u^2 & \Sigma u^3 & \Sigma u^2v & \Sigma u^4 & \Sigma u^2v^2 & \Sigma u^3v \\ \Sigma v^2 & \Sigma uv^2 & \Sigma v^3 & \Sigma u^2v^2 & \Sigma v^4 & \Sigma uv^3 \\ uv & u^2v & \Sigma uv^2 & \Sigma uv^2 & \Sigma uv^3 & \Sigma u^2v^2 \end{vmatrix} \begin{vmatrix} a_0 \\ a_1 \\ a_2 \\ a_3 \\ a_4 \\ a_5 \end{vmatrix} = \begin{vmatrix} \Sigma x \\ \Sigma ux \\ \Sigma vx \\ \Sigma u^2x \\ \Sigma v^2x \\ \Sigma uvx \end{vmatrix} \quad (4)$$

In an application of these transformations to frame No. 1049-07301 which included the Johannesburg area of South Africa, 14 control points were located for a 500 km area correlation and 12 control points in each of the four CCT's comprising the frame for an individual CCT correlation. This exercise gave an indication of the rms location errors that could be expected in producing ground truth overlays for localised and regional geological mapping respectively (Table 1). As each display covered only the area of a single CCT (quarter of full frame), location errors per CCT were more relevant to ground truth correlation than a full frame correlation. Location errors for each of the four CCT's comprising the Johannesburg frame ranged from 50 to 160 meters rms which compared favourably with the 150 meters typical registration accuracy obtained between CCT display separations used to produce colour composites. For a transformation of the full frame, somewhat larger location errors of 219 meters rms (first order) and 182 meters rms (second order) were evident from the transformations (Table 1). Curiously, if the control points of CCT were displaced by 4 pixels in the pixel advance direction the first order transformation error was reduced considerably to 178 meters rms. The adjusted line length in the ID record corresponded to the actual line of the CCT's however. In a test run of CCT-1 using 12 control points and 10 test points, an rms location error of 147 meters was noted for the test point group. This figure was comparable with the registration accuracy of the displays for colour composites.

In comparing the first and second order residual errors (Table 1), the second order fit invariably improved location accuracy over the first order fit. This was noted particularly in the scan advance direction (northing) although a systematic pattern in a vector plot of the residuals was not readily apparent (see figure 2).

Having evaluated the coefficients of a transformation and establishing its accuracy, one useful way of implementing it for ground follow up studies is to produce an overlay of cadastral features. An example of such an overlay composited with band 5 of frame 1049-07301 (CCT1) is shown as figure 1. To produce this black and white composite, the S.A. National Co-ordinates of cadastral intersections were input to the transformation, interpolated in the CCT pixel matrix and appropriate pixels flagged as 50% sensor count in a dummy pixel matrix of zeros. The updated dummy CCT was then displayed as described above and registered with the MSS CCT display with which it had been correlated. This form of overlay was particularly useful in geological studies as not only did it provide an easily recognisable grid of fence positions on a CCT display enlargement (a useful property for ground work in remote areas) but could also provide a basis for planning a new exploration venture. For instance, if a stratagraphic horizon containing sporodic mineralization could be traced under sand cover as a vague trend in a LANDSAT image in areas where it was previously unmapped, it would be important to ensure exactly which farms the horizon appeared to cross before acquiring appropriate exploration options.

GEOLOGICAL APPLICATIONS

As the production of CCT displays was inherently more involved than the photographic printing from NASA 70mm negatives, the approach to the usage of the CCT's was specific to geological problem areas. Such areas in which CCT displays could usefully play a part were found amongst others to be portions of those regions which had undergone metamorphic deformation in the form of complex folding and faulting and in which associated mineralization was to a certain extent structurally controlled. The contribution of CCT displays was noted to be most significant when considered as part of a multi-disciplinary approach to geological exploration.

BASE METAL DEPOSITS OF CENTRAL SOUTH WEST AFRICA

CCT imagery was used as an aid to the understanding of the regional structural controls of recently discovered copper deposits to the east of the city of Windhoek in central South West Africa. This mineralization, which takes the form of massive sulphide bodies, occurs within the Khomas schist (biotite-quartz-felspar schist) sequence of the Damara geosyncline and is associated with a well demarcated zone of amphibolites known as the Matchless Amphibolite belt. Subsequent to the discovery of these deposits on the farms Otjihase, Ongeama and Ongombo West, an extensive program of aerial photography, both ground and airborne geophysical, soil geochemical, and conventional geo-

logical mapping using aerial photographs, was undertaken in an endeavour to ascertain the extent of the mineralization and understand its possible genesis and controls. The essence of the results of these conventional exploration techniques is shown in figure 6a which is a slightly idealized rendition of most of the essential geological and geophysical information in the country around the mineralized bodies.

The geological mapping indicates that the zone of amphibolite, which constitutes a portion of the Matchless Amphibolite belt, is comprised of up to 4 bands of amphibolite. These are traceable from Windhoek to the east but peter out in the vicinity of the Ongeama occurrence and no amphibolite was located to the east of this deposit along strike (Fig. 6a). A northern zone of amphibolite also consisting of a number of bands commences just east of the Otjihase deposit, and continues as a zone of discontinuous and scattered amphibolite lenses which can be traced further east and which occur in more or less the same stratigraphic zone as the Ongombo West occurrence which straddles the White Nossob river (see figure 6a). The amphibolite belt is again traceable to the east of the latter occurrence but is poorly exposed. Thus two major parallel but separate amphibolite zones with an overlap between Otjihase and Ongeama would appear to be present.

A sequence of well banded felspathic quartzites with minor interlayered amphibolite horizons was mapped in the southern part of the area. This sequence trends east-west along most of its strike but swings sharply north in the extreme east where signs of intense folding are apparent in parts. An intrusive granite probably representing a remobilized basement dome was mapped in the extreme south eastern corner (figure 6a) and appears to be partly responsible for the northward swing of the felspathic quartzite sequence in this area.

No distinctive stratigraphic zones could be mapped in the well foliated shallow dipping biotite-quartz-felspar schists which constitute the host rocks for the amphibolite belt.

A number of faults have also been mapped, the set between the Otjihase occurrence and the city of Windhoek being fairly clear (figure 6a). Faults with similar strike directions were also mapped to the east of the Ongeama deposit.

An airborne magnetic survey was subsequently carried out over a portion of the area as depicted in figure 6a. Areas of relatively low magnetic response 3060-3100 gammas and areas of relatively high magnetic response 3120-3180 gammas indicate that the regional structure is complex. Due to the nature of the mineralization (massive pyrite with chalcopyrite, sphalerite and variable amounts of magnetite) all three mineral occurrences give rise to high magnetic responses. In the case of the Otjihase occurrence a clear indication of the plunge of the ore shoot (N.W.) is also apparent. Detailed interpretation of the magnetic pattern has indicated the possibility of a number of faults, additional to those recognized from the geological mapping programme.

A regional soil geochemical programme has also been carried out in the area and as one would anticipate, all the mineral occurrences are associated with anomalous values of copper (above 80 ppm) and zinc. No significant additional geochemical anomalies were obtained in the area.

As 1:1 000 000 scale LANDSAT MSS colour composites had been useful in illustrating the regional geology within the Damara geosyncline (Viljoen et al, 1975) 1:300 000 scale enlargements of all the MSS bands were scrutinized to determine whether fine detail within the imagery could provide structural information supplementary to that given by conventional methods. The region covered in figure 6 is outlined on band 5 of the CCT display (figure 4b). The photointerpretive study revealed that the different MSS bands showed different aspects of the geological picture (fig. 3a, b & c). The resulting composite interpretation of all bands is presented in figure 6b.

The individual mineral occurrences which are represented by iron oxide cappings (gossans) at surface, could not be recognized from the imagery due to their limited size but their positions have been indicated to facilitate description (fig.6b & c).

Slightly darker linear tones to the east of Windhoek and to the east of the Otjihase occurrence represent the narrow amphibolite horizons which constitute a portion of the Amphibolite belt. These are most clearly seen on the band 5 imagery (fig. 3b). No other stratigraphic components can be recognized within the Khomas schists themselves but the well banded felspathic quartzite sequence indicated from the field mapping (fig. 6a) can be distinguished as a well defined belt to the S.E. (fig. 3a, b & c).

Portion of the reactivated basement granite dome described earlier is also discernable by its lighter colour tone on the right hand side of the image. The imagery provides regional structural information particularly with regard to the zone of faulting between Windhoek and Otjihase. Thus, although small-scale detail is not as clear, the imagery adds significantly to our previous knowledge of the geology and regional structure of the area but is not definitive enough to reach any firm conclusions.

Examination of the CCT imagery however indicates that this product has substantially more definition and provides data which has added substantially to our knowledge of the regional geology and structure of the area.

All the elements distinguished on the NASA photographic products are clearly seen and in all cases are enhanced due to the better definition of the CCT displays (fig. 4a, b & c). A map based on the interpretation of all CCT produced bands as well as ratiod bands is depicted in figure 6C.

Study of the imagery reveals that the amphibo-

lite belt can be traced over a relatively greater distance from Windhoek in an easterly direction where it disappears in the vicinity of the Ongeama gossan. Although not as clear, the amphibolite belt can again be seen to the east of the Otjihase gossan and towards the Ongombo West occurrence, disappearing in an easterly direction. This confirms the geological mapping which revealed a duplication of the amphibolite belt. As in the case of the NASA imagery the resolution is not sufficient to indicate individual gossans but their positions have been indicated on the interpretation to facilitate descriptions.

The well layered felspathic quartzite sequence described above is clearly defined to the south where the major structural disturbance of the stratigraphic trends, taking the form of a sharp swing north and accompanied by folding, can be seen on the right hand side of the image (fig. 4a, b & c). To the north, fairly regular trends are once more encountered and there is a strong suggestion of one or more zones of structural disturbance running approximately NE - SW approximately along the course of the Otjihase river (fig. 6c).

Part of the dome of reactivated basement granite is also clearly discernible by its lighter colour tone on the right hand side of the imagery (fig. 4a, b & c).

The imagery provided a large amount of unique regional structural information only part of which was apparent from the interpretation of the NASA products (compare fig. 6b & c).

The zone of faulting between Windhoek and Otjihase is particularly clear, and although the dominant fault direction is NNW - SSE there are also strong N.W. and N.E. components as well.

Some of these faults clearly displace the amphibolite belt apparently by en echelon movement in the region to the east of Windhoek. Numerous other faults are also apparent, particularly in the area to the south east of the Otjihase deposit (see figure 6c and central portion of figure 4a, b and c). While most of the fault traces appear to form fairly high angles with the schistosity of the Khomas Series and have in many instances been accentuated by the drainage pattern, other evidence suggests the presence of a number of older fault zones probably in the form of wrench or thrust faults with the fault traces being close to the schistosity of the Khomas schists and therefore not as readily apparent.

Of particular interest is the evidence for one or more major early thrust or wrench faults with left lateral movement and with attendant minor folding (referred to above) which were responsible for the probable displacement seen in the layered felspathic quartzite sequence and in the displacement and partial duplication of the amphibolite belt. One branch of this system of early faulting appears to follow the Otjihase river while the other which has been displaced in part by the younger faults, occupies a zone more or less between the Otjihase and Ongeama occurrences continuing in an easterly direction, and merging with the fault described above (fig.6c).

Further evidence for the presence of this zone of dislocation is provided by a zone of good outcrop with dark tones and conspicuous linears, within the Khomas Series and lying to the S.E. of the Otjihase gossan (see figure 4a). The same tone is to be seen to the north between the Otjihase and White Nossob rivers and this distribution pattern suggests displacement of some type of stratigraphic component within the Khomas Series by the wrench faulting referred to earlier.

Ratiod CCT imagery is presented in figure 5a,b and c and although not adding significantly to the data content, a number of points are worthy of note. Drainage patterns which are largely controlled by faulting in the area are particularly enhanced in figure 5a (5/7 ratio) where the waterways are manifested as dark tones. Figure 5b (4/7 ratio) gives a clear indication of the probable trace of one of the thrust faults referred to above as well as of the behaviour of stratigraphic trends within the felspathic quartzite sequence.

This study has illustrated the use of CCT produced imagery in convincingly indicating probable underlying regional structure in the general area of three base metal occurrences. Although providing the essential information concerning the geology of the area, conventional techniques were not able to convey the same regional tectonic insight into the area as the CCT imagery has done.

THE N.W. CAPE PROVINCE, SOUTH AFRICA

The N.W. Cape Province of South Africa provided a further example of the practical advantage of ERTS-1 imagery (produced from NASA negatives) in providing a regional geological framework as a guide to a mineral exploration programme in a largely unmapped terrain (Viljoen, 1974; Viljoen et al, 1975).

From the point of view of competitive mineral exploration it was essential that an insight into the regional geological controls of the base metal mineralization of the area be obtained as rapidly as possible.

Eight ERTS-1 colour composite images were consequently enlarged to a scale of 1:500 000 and were used in the compilation of such a regional geological map.

In order to gain a better understanding of the structure and stratigraphy of the environs of two of the more important base metal deposits, studies were made of 1:300 000 enlargements from NASA 70mm positives and CCT displays including the ratio imagery of bands 5/7, 4/7 and 4/5.

Figure 8b illustrates a composite interpretation of the 4 MSS bands and ratio imagery while figure 7b represents the composite interpretation of the 4 MSS bands of the same scene from NASA 70mm positives.

The entire area covered by this scene is underlain by a variety of folded paragneisses. The more quartzitic components of these gneisses are of considerable

importance with respect to the base metal mineralization of the area. In the flat plain to the south of the Orange river the quartzitic zones generally stand out in marked relief to the surrounding country and are to be seen in the south and central portions of the scene under consideration. The internal structure and definition of these quartzitic hills is particularly clear from the CCT displays of bands 5,6 and the ratio of bands 5/7 as opposed to the individual bands from the NASA photographic products (compare figures 7b and 8b).

Although the quartzites are not developed in the vicinity of the Orange river to the north, the erosive action of the waterway has etched out the structure of the paragneisses adjacent to the river. Interpretation of the geology has indicated the presence of a major wrench dislocation within these gneisses and lying just north of the river (fig. 7b and 8b). The right lateral sense of movement of this fault is revealed by drag in the paragneisses lying to the north and south of the wrench fault, while the linear aspect of this structure is marked by a well defined zone of shearing which can be traced for a distance of 450 kilometers along strike to either side of the zone shown in figures 7 and 8.

A number of large intrusive mafic bodies as well as numerous smaller bodies have been emplaced along this structural dislocation two of the larger ones being clearly seen on the imagery. Continued movement after the emplacement of the mafic bodies is indicated by the conversion of most of the intrusive to amphibolites.

Besides the major wrench fault a number of other lineaments, representing both faults and other linear features, are also to be seen on the imagery, the wealth of added data from the CCT presentation being apparent from a comparison of the interpretations (figs. 7b and 8b). A NNE - SSE direction is the most prominent but a N - S and an ENE - WSW set is also apparent (fig. 8b). In a similar way areas of thick sand cover are more clearly defined on the CCT imagery, band 4 being particularly useful for the mapping of this parameter. Examples of band 4 from NASA negatives and CCT products is given in figure 7a and 8a respectively and clearly illustrates the superior data content of the CCT product. A number of sand dunes not obvious from the interpretation of any of the NASA negatives are clearly seen on the CCT products, particularly on band 5.

Colour composite presentations of NASA negatives and CCT products are shown as figures 9 and 10 respectively. Study of these images indicates the greatly superior data content of the CCT colour composite in all aspects of the geology and the advantages of this type of product to geologists is obvious.

Thus although important information can be gained from the interpretation of the photographic products, the detail apparent from the interpretation of individual CCT bands and ratiod bands, is considerably greater and gives a far better appreciation of the regional structure of the area.

It is concluded that if used in the correct context and in specific areas where information regarding regional structure and stratigraphy is required in a particular exploration or geological problem, CCT produced imagery will certainly become a more and more useful tool. If the method can be developed on a routine basis then it will be possible to gain a quick regional geological understanding of numerous prospect areas in a very short period of time thus conceivably avoiding a number of unnecessary steps and hence expenditure, in future exploration programmes.

ACKNOWLEDGEMENTS

The authors wish to acknowledge the contribution of Mr. B.P. Gilbertson in the early stages of this work and the invaluable computation system of Mrs. J.A. Trollip.

REFERENCES

Colvocoresses, A.P. "The Map Projection of the ERTS Multispectral Scanner". Proc. of the ASP 40th Annual Meeting. p. 607. (1974).

Kreitzer, M.H. "Direct Additive Printing". Photogrammetric Engineering. Vol. XL, No. 3. pp. 281 - 286 (March, 1974).

Laboratory for Agricultural Remote Sensing, Purdue University. "Remote Multispectral Sensing in Agriculture". Annual Report Res. Bull. No. 844. Vol. 3 (September).
also: Remote Multispectral Spectral Sensing in Agriculture, 1,4.

McEwan, R.B. and Asbeck T.A. "Analytical Triangulation with ERTS". Proc. of ASP 41st Annual Meeting (March, 1975).

Nagy, G. "State of the Art Pattern Recognition" Proc. IEEE, 56, pp. 836 - 862 (1968).

NASA, "ERTS Data Users Handbook" NASA, Goddard Space Flight Center, Greenbelt. Md. (1972).

Skoonmaker, J.W. "Geometric Evaluation of MSS Images from ERTS-1". Proc. of ASP 40th Annual Meeting (March, 1974). pp. 582 - 588.

Viljoen, R.P. "ERTS-1 Imagery as an Aid to the Understanding of the Regional Setting of Base Metal Deposits in the North West Cape Province, South Africa. Third ERTS Symp. (Dec. 1973).

Viljoen, R.P.; Viljoen, M.J.; Grootenboer, J. and Longshaw, T.G. "ERTS-1 Imagery : Applications in Geology and Mineral Exploration". Miner. Sci. Engng. Vol. 7. No. 2 April, 1975.

Vincent, R.K. "Ratio Maps of Iron Ore Deposits Atlantic City District, Wyoming". Symp. on Significant Results from ERTS-1 (March, 1973). Paper G16, Vol. 1.
also: "Spectral Ratio Imaging Methods for Geological Remote Sensing from Aircraft and Satellites". Symp. on Management and Utilization of Remote Sensing Data. Sioux Falls (October, 1973).

TABLE

TABLE 1 : RMS LOCATION ERRORS FOR SECTIONS OF FRAME NO. 1049-07301

FRAME NO. 1049-07301		Root-mean-square location errors calculated from transformation residuals			
Arial Extent of Fit	Number of control points	Byte advance direction (x) in meters		Scan advance direction (y) in meters	
		1st Order	2nd Order	1st Order	2nd Order
500 km^2 of CCT 1	14	41	41	39	38
Total area of: CCT 1	12	54	35	60	43
CCT 2	12	109	100	105	43
CCT 3	12	35	29	156	35
CCT 4	12	87	73	47	49
Full Frame	48	184	151	119	90
Test case using 12 CCT 1 control points and 10 test points	12	97	-	111	-

Fig. 1. Part of CCT-1 of frame No. 1049-07301 showing composited cadastral features as white lines. Scale approximately 1:500 000.

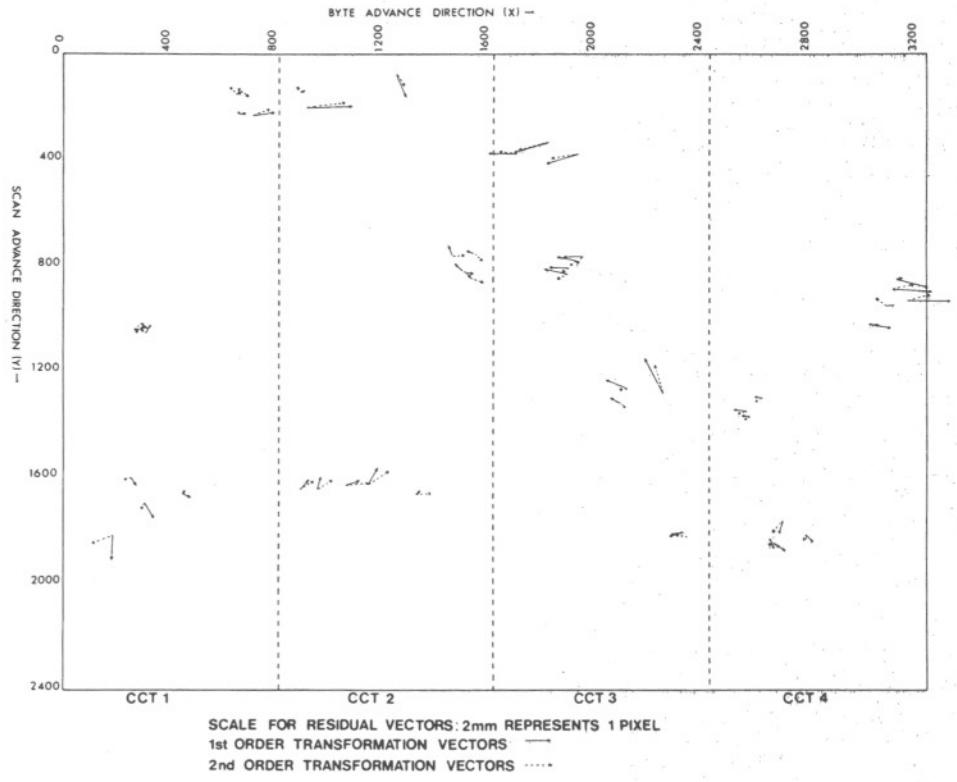

Fig. 2. Plot of first and second order transformation residual vectors for full frame correlation of frame No. 1049-07301

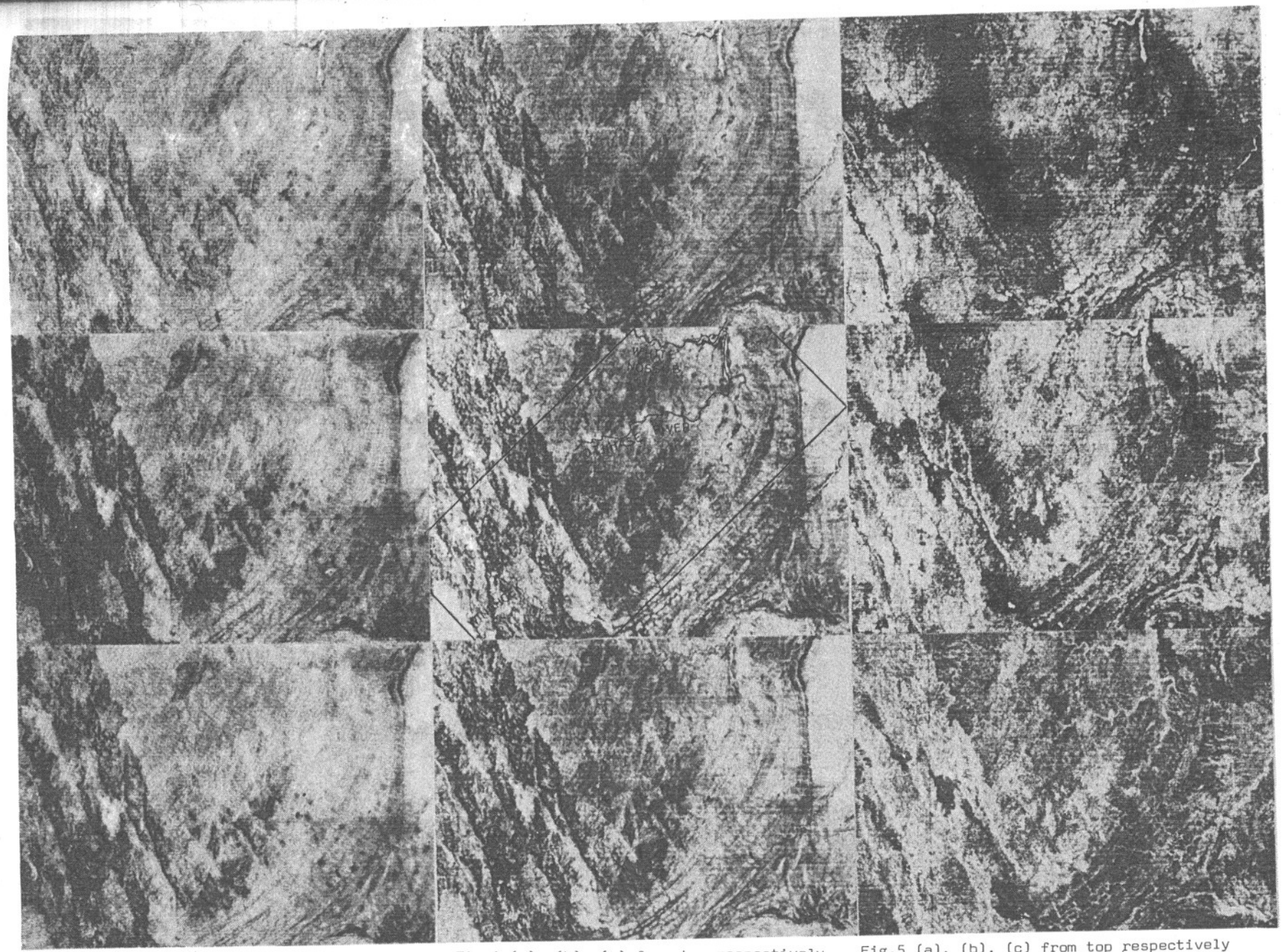

Fig.3 (a),(b), (c) from top respectively Bands 4, 5, 7 printed from NASA 70mm. positives.

Fig.4 (a), (b), (c) from top respectively Bands 4,5,7 printed from CCT displays.

Fig.5 (a), (b), (c) from top respectively ratio images of Bands 5/7,4/7,4/5 from CCT's.

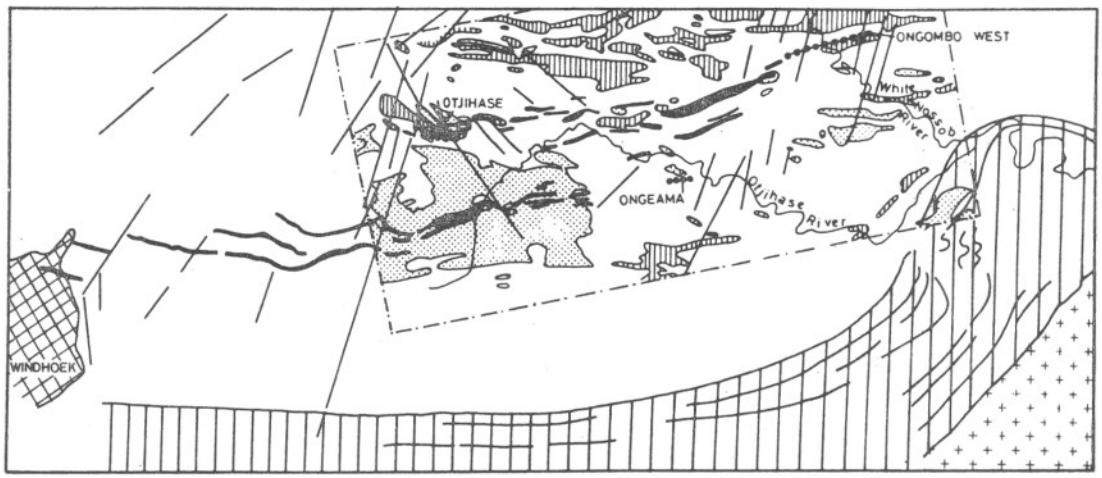

Fig.6 (a). Available geological and geophysical data around the Otjihase, Ongeama, and Ongombo West base metal deposits prior to interpretation of LANDSAT imagery.

Fig.6 (b). Interpretation purely from individual MSS bands produced as black and white prints from NASA 70mm positives.

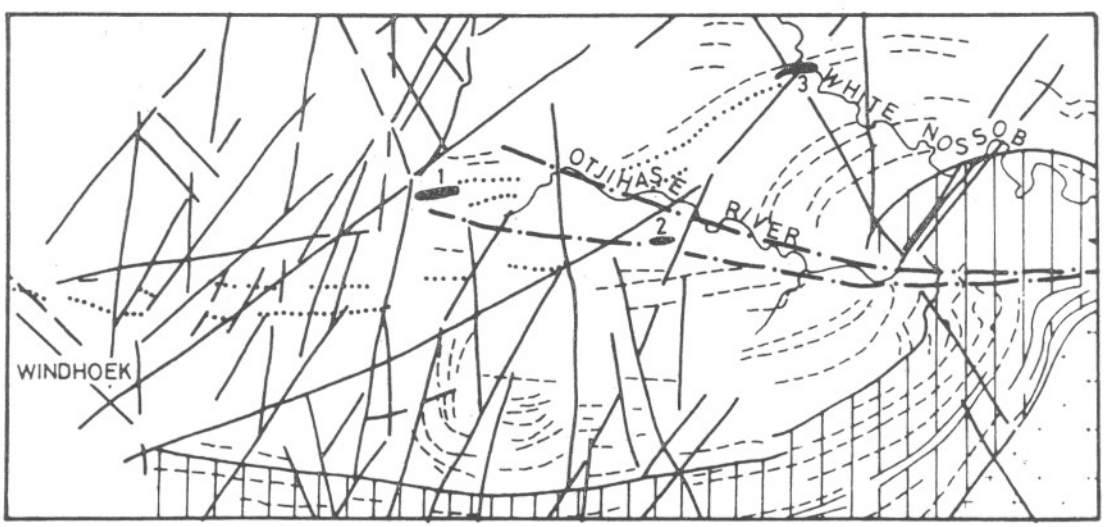

Fig.6 (c). Interpretation purely from individual MSS bands produced as black and white prints from CCT displays.

Fig. 7(a), (b) and (c) respectively Band 4 (left), Band 5 (right), and interpretation from all bands (centre), generated from NASA 70mm. positives

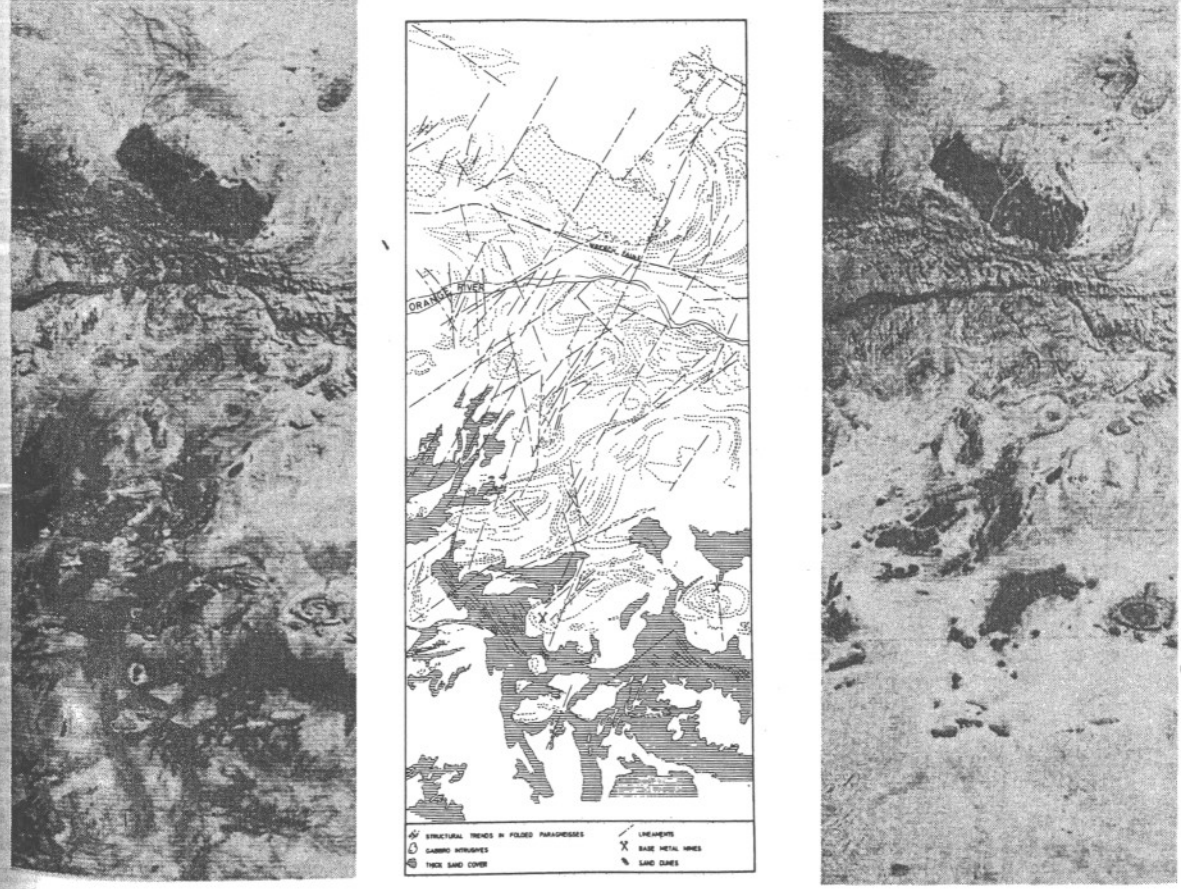

Fig. 8(a), (b) and (c) respectively Band 4 (left), Ratio of Bands 5/7 (right), and interpretation from all bands (centre), generated from CCT displays

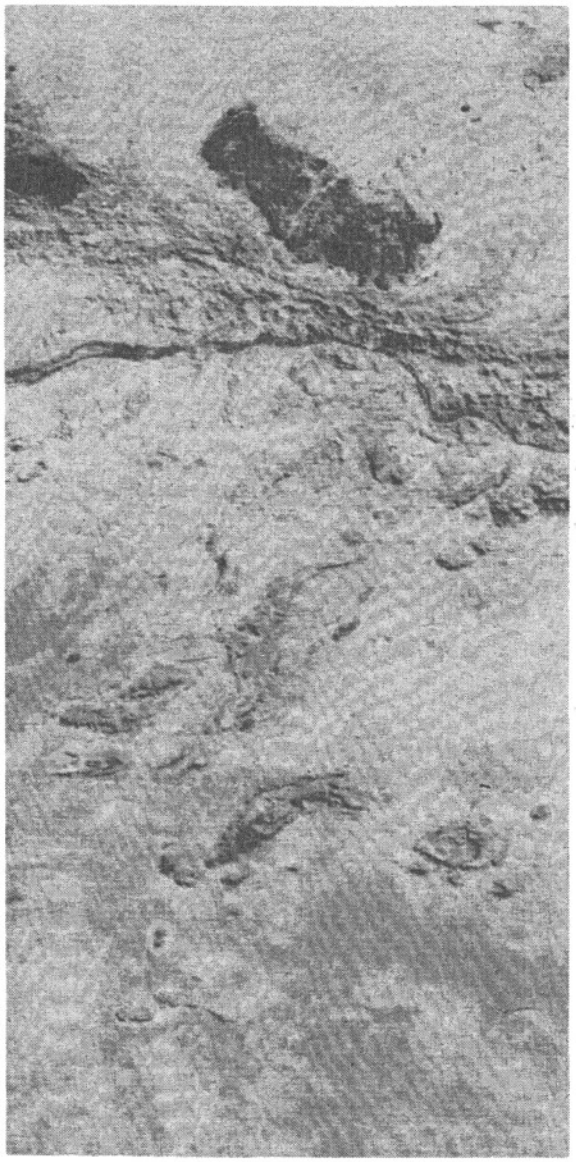

Fig. 9. Colour composite from NASA 70mm positives of bands 4,5 and 7 printed as blue, green and red respectively. Scale approximately 1:500 000.

Fig. 10. Colour composite from CCT displays of bands 4, and 6, and the ratio image of bands 5/7 printed as blue, green and red respectively. Scale approximately 1:500 000